

where the q_{s_i} are charges on the insecticide atoms, q_r is the charge on the receptor, D_{rs_i} the distance between charges, k a constant which includes the reciprocal of the dielectric constant, and C a constant taking into account interactions other than the electrostatic binding. We have evidence² that the compounds all act at the sodium channel of a nerve membrane but no detailed information concerning the receptor charge distribution. We therefore approximate the above equation by assuming that all receptor factors are constant. Thus

$$\log LD_{50} = A \sum_i q_{s_i} + C,$$

where A is assumed constant. Now $\sum_i q_{s_i} = 0$ for neutral molecules if the summation is taken over all the atoms. However, since the model postulates two distinct parts of the 'molecular wedge' we have taken the sum over the part containing the two aryl rings and the bridging atom only and placed the balance of the charge on the apex. The results are summarized in the Table. A straight line of best fit through the points has a correlation coefficient of 0.998.

This finding is in accord with the effects² of substitution in the aryl rings on the negative coefficient of temperature with insect mortality. This was found to be independent of the chemical nature of the apex of the insecticide, for compounds of similar steric features which fit our model.

We consider the results of this work promising enough to continue calculations with more compounds and more accurate molecular orbital methods.

Zusammenfassung. Neues Verfahren mittels Molekular-orbital-Berechnung zur Vorausermittlung der chemischen Konfiguration und Wirksamkeit von Insektiziden vom Typ des DDT.

G. HOLAN and T. H. SPURLING⁸

CSIRO Division of Applied Chemistry, P.O. Box 4331, Melbourne (Victoria 3001, Australia), 5 November 1973.

⁸ The authors thank Dr SHIFF for supervizing the entomological testing and Mr C. T. F. VIRGONA for biological work.

A Study of the Combined Raman and Fluorescence Scattering from Human Blood Plasma

Raman spectroscopy has experienced a revival during recent years due to the utilization of lasers for excitation. It has thus been possible to extend this technique to studies on the conformation of complex organic molecules in aqueous solutions, such as proteins (LORD and YU¹). It seemed therefore possible that new information on the physical structure of the dominating constituents of blood plasma might be obtained. In connection with such studies we observed that the overlapping fluorescence scattering shows features which seem to be of clinical importance.

The weak intrinsic fluorescence of blood plasma, which is of the same order of magnitude as the Raman scattering, has not been examined earlier, so far as we know. Laser light excitation at different wavelengths were used, and we found that the combined fluorescence and Raman spectra in the region 542 nm–648 nm are particularly interesting. The spectra are thus changed in a regular way at various diseases, as will be described below.

Plasma samples from patients suffering from different organic diseases with definitely settled diagnoses were

analyzed: lues, erysipelas, mycosis fungoides, viral hepatitis, sepsis, leucemia, and advanced carcinoma with metastases and different primary site. Healthy controls of both sexes covering all age groups were also analyzed. After an overnight fast of at least 12 h, samples of venous blood were taken. The blood was collected in standard heparin tubes (Vitrum). After centrifugation for 10 min at 2500 g, 0.1 ml plasma was injected into a glass capillary, diameter 0.1 mm, by careful avoiding formation of air bubbles.

A Cary 82 spectrophotometer with an argon laser was used. The capillary was adjusted in the centre of the unfocused green line (514.5 nm), with the axis of the capillary parallel with the beam. It was tedious work to adopt the experimental running conditions, so that reproducible spectra could be obtained. The laser power finally used, measured at the sample, was 150 mW. Fluorescence maxima and broad Raman bands, such as

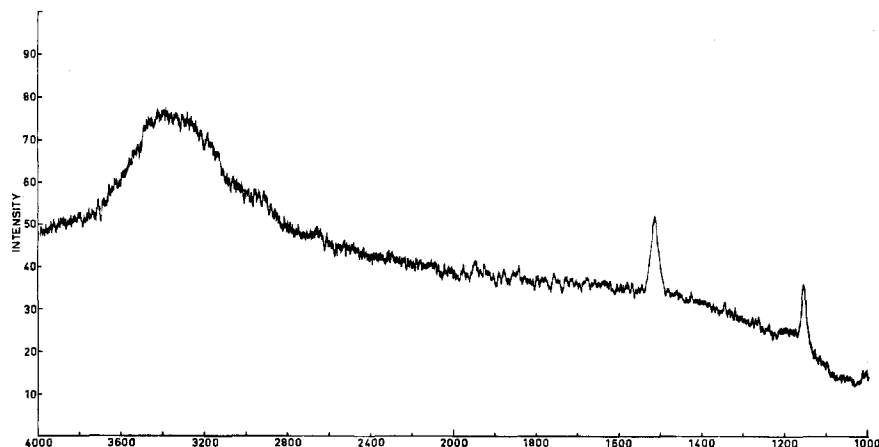


Fig. 1. Spectrum from a healthy woman, age 23. No history of any disease. Routine hematological and urinary analyzes normal.

¹ R. C. LORD and N.-T. YU, J. molec. Biol. 50, 509 (1970).

that of O-H stretching vibrations, could be separated by use of different excitation wavelengths (the 514.5 and the 488 nm lines). The fluorescence effects which could be correlated with diseases were, as mentioned earlier, most pronounced in the range 542–648 nm. This corresponds to a Raman spectrum in the range 1000–4000 cm^{-1} with excitation by the 514.5 nm line.

The standard types of clinical blood analyses were performed for correlation with Raman and fluorescence scattering data.

After the ideal running conditions described above had been reached, it was soon revealed that spectra from healthy individuals were very similar, whereas diseased states showed various deviations. The spectra were reproducible after several months in the same individual

during a constant stage of health or disease. A typical spectrum from a healthy individual, shown in Figure 1, is characterized by the following features: a) Strong Raman scattering bands at 1160 and 1520 cm^{-1} due to resonance enhanced conjugated systems of C-C single and double bond stretching vibrations², and a weaker Raman scattering band at 1010 cm^{-1} due to C-C stretching vibration from aromatic protein side chains. b) A maximum in the spectrum formed by Raman scattering corresponding to the broad O-H stretching vibration band at 3400 cm^{-1} (dominating due to the high water content) and the unresolved N-H stretching vibration band at about 3300 cm^{-1} . A broad shoulder at about 2900 cm^{-1} due to the C-H stretching vibration band is also seen. c) Background fluorescence scattering characterized by moderate slope upwards in the range 1000–1600 cm^{-1} , and a horizontal niveau or a slight slope upwards in the range 1600 to 2800 cm^{-1} . The spectra of all normal cases obeyed the conditions mentioned.

In the combined recording of Raman and fluorescence scattering of the plasma from diseased individuals of our material, we observed strong changes in the background spectra due to changes of the intrinsic fluorescence. Some common general characteristics in the spectra not observed among healthy persons, and therefore defined as pathological, were as follows: a) increased slope upwards of the background scattering curve in the range with the

Comparison between the present spectral information and ESR

	Healthy patients (13)	Diseased patients (53)
Normal* ESR	13	21
Pathological ESR	0	32
Normal spectrum	13	0
Pathological spectrum	0	53

*Males: age <50: 0–13 mm/h; age \geq 50: 0–20 mm/h. Females: age <50: 0–20 mm/h; age \geq 50: 0–28 mm/h.

² E. M. POPOV and G. A. KOGAN, *Opt. Spectrosc.* 17, 362 (1964).

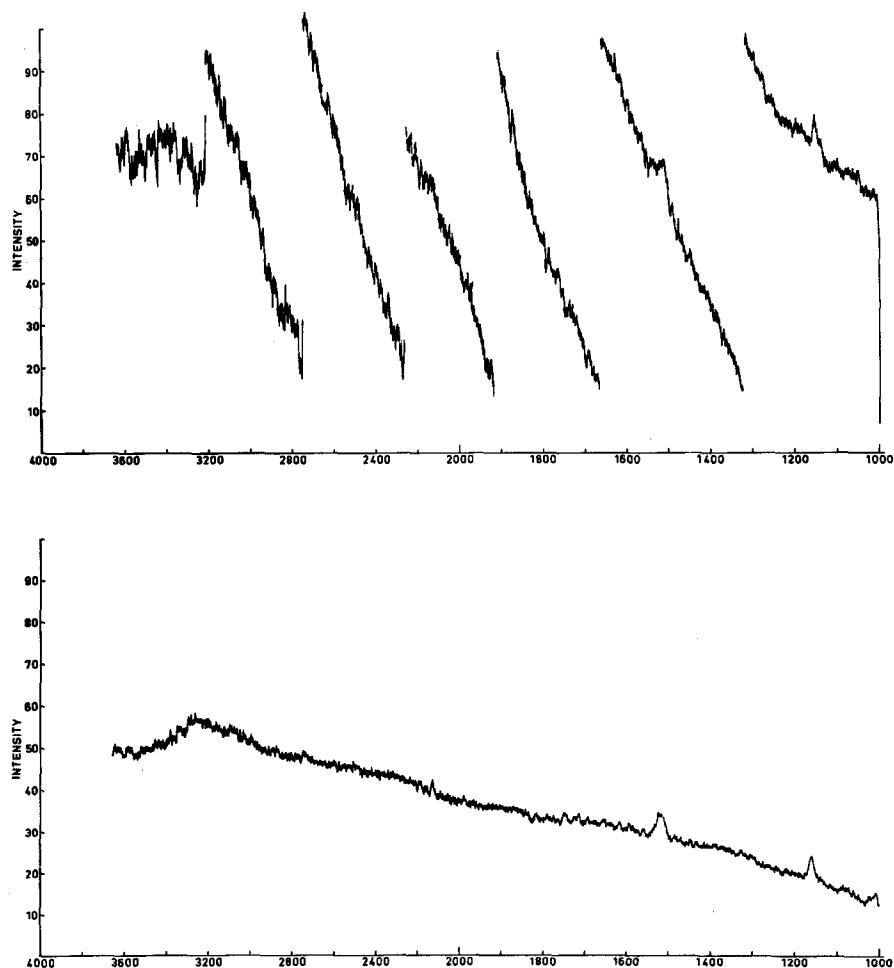


Fig. 2. Changes in the spectrum from a diseased state to a healthy state in a patient with hepatitis. The spectra were obtained from a 20-year-old woman, with homologous serum hepatitis. The spectrum above was recorded during the icteric period, and a new spectrum (below) was taken 20 days later when the patient had clinically recovered and routine liver function tests were normal except for the thymol turbidity test (0.48).

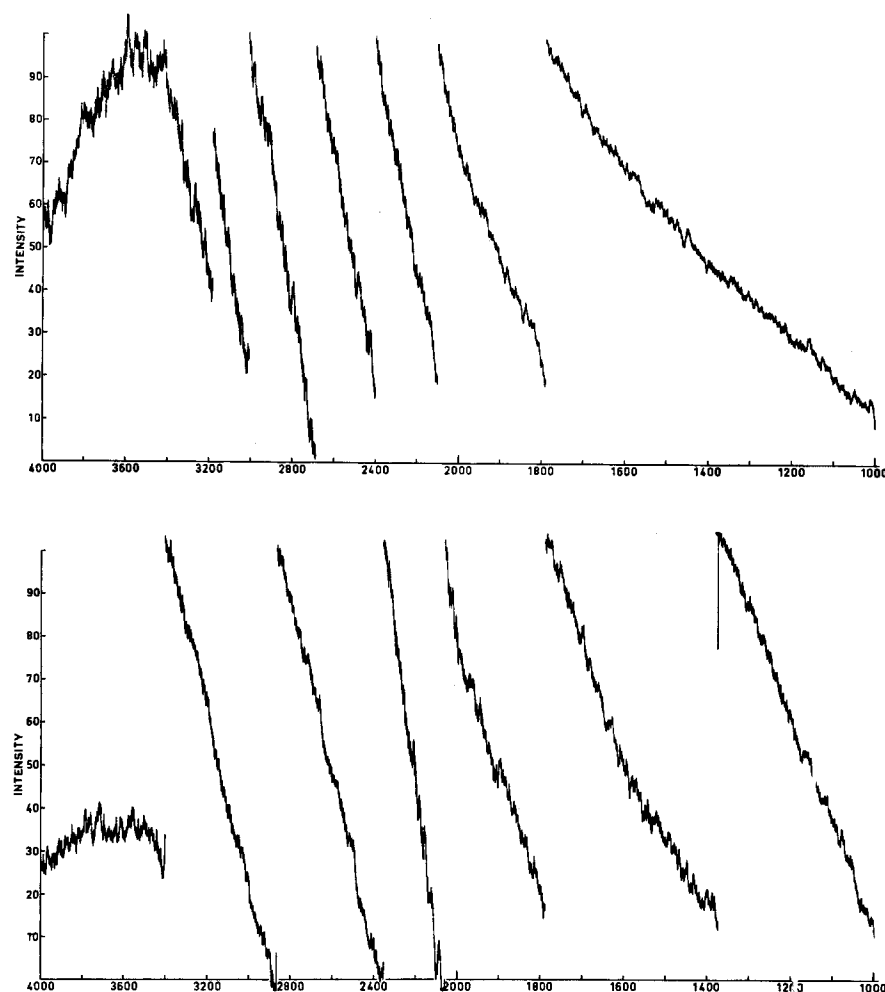


Fig. 3. Characteristic pathological spectra. The spectrum above was obtained from a woman, age 62, with infiltrating mammary carcinoma, grade II. The spectrum below was obtained from a 64-year-old woman, with pseudomucinous papillary cystadenocarcinoma.

maximum formed by the Raman O-H and N-H stretching vibration band (about 3400 cm^{-1}). b) A strong slope upwards of the curve in the range $3600\text{--}4000\text{ cm}^{-1}$ (fluorescence maximum above 4000 cm^{-1}) or a broad fluorescence maximum at about 3900 cm^{-1} ; c) the normally very weak C-H band near 2900 cm^{-1} forms a pronounced maximum in the curve (this feature could always be correlated with pathologically high lipid content).

Two examples of pathological spectra are presented in Figures 2 and 3. The spectrum in Figure 2 illustrates how the curve is normalized when the patient gets healthy. Patients with hepatitis always showed a steep slope with a maximum below 4000 cm^{-1} (type a) above). All patients with advanced carcinomas showed such a steep slope due to strong intrinsic fluorescence that the sharp Raman bands at 1160 and 1520 cm^{-1} did not even show up in the spectra (see Figure 3).

Numerous conventional fluorescence spectroscopy studies have been reported utilizing the fluorescence of blood plasma constituents. It is, for example, known that the presence of peroxidizing lipids in plasma modifies the fluorescence of serum albumin³. The various spectra reported do not, however, show any of the details discussed above, as the sensitivity in recording fluorescence spectra are several orders of magnitude lower. The changes in the spectra observed do not seem to be very specific with regard to disease according to the present experimental material.

A comparison in 66 randomly selected individuals in our material with the combined Raman and fluorescence scattering indicate that the recorded spectra are superior to the dominating clinical screening method; measurement of the erythrocyte sedimentation rate (ESR). (See Table). It thus seems as if the recorded combined Raman and fluorescence scattering spectra are very sensitive for various pathological disturbances affecting the plasma. The main function of the Raman bands in these spectra is to provide a calibration of the weak fluorescence scattering.

Zusammenfassung. Mit Laserstrahlen angeregte Raman- und Fluoreszenzspektren im Blutplasma gesunder und mit verschiedenen Systemerkrankungen behafteter Frauen und Männer werden mit der Blutsenkungsreaktion korreliert, wobei sich Unterschiede zwischen normalen und pathologischen Fällen zeigen.

K. LARSSON and L. HELLGREN

Lipid Chemistry Laboratory and Sahlgren's Hospital, University of Göteborg, Kraketorpsgatan 20, S-431 33 Mölndal (Sweden), 31 October 1973.

³ B. L. FLETCHER and A. L. TAPPEL, *Lipids* 6, 172 (1971).